International Journal of Science and Research (IJSR)
ISSN: 2319-7064
SJIF (2022): 7.942

Correction of THz Images for Trustful Identification of Library of Materials in Reflection Configuration

Li-Wei Hsu[1], Maxime Bernier[2], Emilie Herault[3], Frédéric Garet[4], Olivier Lavastre[5]

[1, 2, 3, 4, 5]IMEP-LAHC Laboratory, Savoie Mont Blanc University, CNRS, Grenoble Alpes University, Grenoble INP, Scientific Campus, 73370 Le Bourget du Lac, France

[5]Corresponding author Email: *olivier.lavastre[at]univ-smb.fr*

Abstract: ***Terahertz multispectral imaging is an emerging technique for material identification, as many molecules present unique spectral signatures in the frequency range that typically spreads from 100 GHz up to several THz. In most cases, samples to identify are imaged in transmission, which is most of the time not the appropriate configuration regarding industrial requirements. Unfortunately, in reflection configuration, the sample thickness leads to terahertz beam misalignment (defocusing, lateral shift…) that involves erroneous estimation of the reflected amplitude. Such misalignment prevents any absolute characterization of the sample under testing. Thus, to evaluate libraries of materials, one must prepare samples showing exactly the same thickness. This process could be extremely time-consuming and very often, not applicable for fast evaluation in the industry. In this paper, we propose a novel method that evaluates the effect of the unwanted misalignment artifacts, due to the varying sample thickness. Such a method is applied to correct the THz amplitude image and to get an absolute image in reflection configuration, in order to compare library of materials whatever the sample thickness. Article highlights: Misalignment induced by thickness variation, Direct measurements using THz reflection spectroscopy, Accurate and fast comparison of samples with different thicknesses, New method to evaluate material library.***

Keywords: HTE High Throughput Experimentation**,** THz, reflection imaging, accurate comparison, misalignment correction

1. Introduction

Nowadays, THz imaging spectroscopy is largely applied in different applicative fields such as biology [1], the pharmaceutical industry [2], food inspection [3], explosives detection [4], automotive inspection [5], material detection and identification [6], or environmental monitoring [7]. In order to accelerate analysis speed, there is a strong interest in developing parallel analysis methods, instead of performing individual experiments one by one. In this context of fast experiments, the high throughput experiment (HTE) is a well-established method [8]. HTE was efficiently applied in the optical domain, such as UV or visible spectroscopy, not only for the fast discovery of innovative materials [9], but also to study their corresponding physicochemical properties, like rheological [10] or adhesive properties [11]. However, for an accurate comparison between analytical data, it is mandatory to use only flat samples showing the same thickness, and particularly if optical methods are used, such as, analysis based on contactless Raman spectroscopy [12] or on fluorescent properties of light emitting diode films [13]. Preparation of samples with the same geometry, i.e. shape and thickness, is really time-consuming. The possibility to investigate a large number of samples without thickness consideration could be really useful for users. We report here a new algorithm based on THz Time Domain Spectroscopy (THz-TDS) results, in order to make reliable THz images, whilst taking into account only the amplitude of the THz pulse [14]. Such a technic allows us to probe a very broad band spectrum, from typically 0.1 THz, up to several THz, through a single measurement of a picosecond electromagnetic pulse.

This technic has been initially developed to characterize materials *i.e.* to measure the dispersion of the complex refractive index $\tilde{n} = n - i\kappa$ of a material over the corresponding frequency range [15]. The imaginary part κ, called extinction coefficient, is related to the absorption coefficient α of the material, while its real part n rules the velocity of the terahertz electromagnetic wave in the sample. When launching a picosecond electromagnetic burst, with spectral components spread typically from 0.1 THz to typically several THz, the pulse transmitted by the sample is shifted in time, distorted and attenuated because of the material dispersion and absorption. By making the ratio of the spectrum of the transmitted pulse, obtained by the Fast Fourier Transform (FFT) time domain measured signal transmitted by a sample, to the FFT of a reference signal without sample, the frequency dependent complex transmission coefficient $\tilde{T}$ of the sample under test is calculated. Finally, the complex refractive index can be numerically extracted from $\tilde{T}$[16].

By repeating this extraction process on different parts of the sample under test (raster scanning), we can rebuild the image of the sample and have spectral information for each pixel: it is the so-called THz multispectral image. This imaging process can either map the refractive index or the absorption coefficient at any available THz frequency, and can be performed in transmission as well as in reflection configuration. In the latter case, the complex refractive index is analytically calculated from the complex Fresnel reflection coefficient$\tilde{R}$, according to equation (1), which can be written for a reflection under anincidence angle $\theta_i$and for a TE polarization [17]:

$$\tilde{\mathrm{R}}(\theta_i) = \frac{\sqrt{\tilde{n}^2 - \sin^2\theta_i} - \cos\theta_i}{\sqrt{\tilde{n}^2 - \sin^2\theta_i} + \cos\theta_i} \quad (1)$$

Regardless of the experimental configuration (transmission or reflection), imaging the optical properties of samples in the spectral domain requires time-consuming pre-processing (FFT of the waveforms for each pixel), and post-processing

to extract precisely *n* and κ. In addition, this later processing suffers from miscellaneous experimental conditions [18-19] that could lead to erroneous images, unless they are considered or corrected by sophisticated and time-consuming algorithms [20-21]. For the sake of speed, simplicity and reliability, all of which are mandatory for reliable identification of library of materials for industrial applications, we propose an empirical imaging method based on the peak-to-peak amplitude measurement of the reflected THz waveforms, associated with a simple correction algorithm.

2. Samples under test and experimental setup description

Sample materials such as glucose, maltose and polyethylene were studied in the experiment; we used "compressed" powder materials in order to get flat-face plain pellets. The pellets were fabricated using a 13mm diameter mold and a pressure of 10 tons. For the sample preparation, maltose and glucose powder were weighed on an electronic scale (100, 200, 300, 400, 500, and 600mg), to get six flat-face plain tablets with different thicknesses.

The THz images were obtained using a *Teraflash pro* THz-TDS system, developed by the TOPTICA company. We used the system in a reflection configuration at a non-normal incidence (incident angle of 8°), that provides a useful spectrum from 0.1 THz up to 3 THz. For the reference measurement, we used a stainless-steel plate that completely reflects the THz signal and that also serves as a holder to put the samples in. We chose a 70 picosecond measurement time window in order to be able to measure sample pellets with thicknesses up to 3 mm with sufficient signal to noise ratio. This way, we record the main reflected THz pulse as well as the first echo induced by the sample. The image of a 13 mm diameter sample contains 530 pixels. For each pixel, we measure the temporal shape of the THz pulse that contains all the spectral information of the material. The distance between 2 pixels corresponds to a sample shift of 0.5 mm. An algorithm written with MATLAB is used to ease the process on matrix calculations and data visualization and to plot the images.

3. Results and Discussion

3.1 Impacts of thickness on amplitude signals

Fig. 1 shows images of 6 pellets made of pure maltose, based on the measurement of the THz reflected signal amplitude. As can be seen on the upper part of the figure,each pellet has a different thickness.

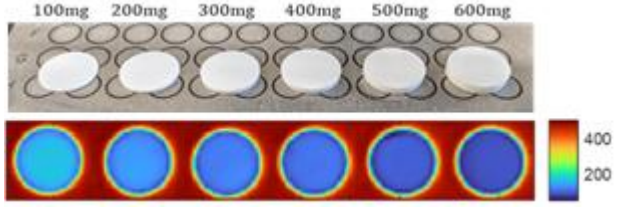

Figure 1: Pure maltose pellets with different thicknesses (upper figure) and the corresponding images base on the reflected THz signal amplitude (lower figure).

We can see on these bare THz images (lower figure), *i.e.* with no correction applied, that the measured amplitudes differ when the sample thickness varies (the blue color representing the amplitude values is not the same from one sample to the other). This result is not coherent as all the samples are made of pure maltose. The sample's refractive indexes are therefore the same, and according to equation (1), the reflected THz amplitude should be the same for all pellets. By taking a closer look at the time domain graph for only one pixel of the image (see Figure 2), we can see some interesting results.

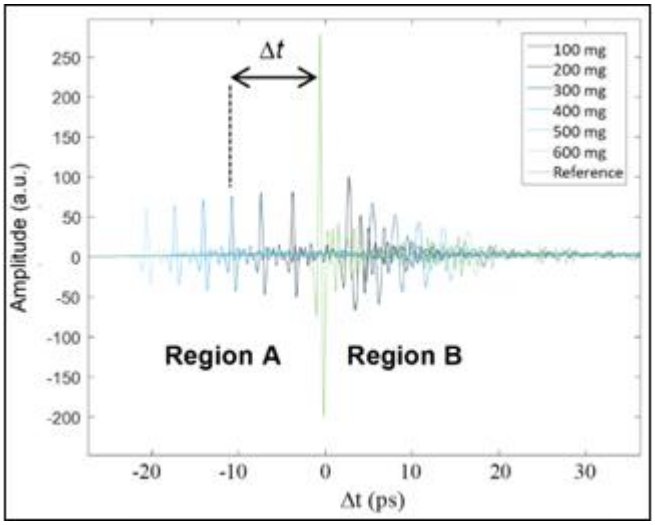

Figure 2: Amplitude of the THz time domain signals reflected on maltose pellets with different thicknesses and the reference signal (arrow).

The time domain signatures of each sample, exhibit two pulses (regions A and B on Fig. 2), as schematically illustrated in Fig. 3. The first one (region A) corresponds to the reflection at the upper surface of the sample under testing. This pulse does not penetrate the sample and the time flight of the THz pulse is shortened as the sample gets thicker: this reflected signal appears earlier than for the reference signal.The second one (region B) corresponds to the reflection at the back side of the pellet, after the THz pulse has passed through the sample twice. As the THz wave travels slower in the material than in the air, the pulse appears later than the reference one.

We can notice that such a phenomenon is at the origin of multiple inner reflections (echoes) that would appear in the waveform (theoretically an infinity of echoes), but the chosen 70 ps measurement time window only allows us to record the first two pulses regarding sample thickness i.e. the pulse reflected at the upper surface and the first echo.

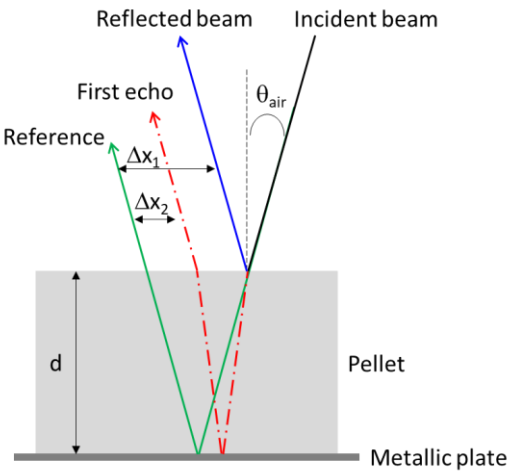

Figure 3: Theoretical representation of THz pulse interaction with the sample in a reflection configuration.

It is interesting to note that since the first pulse does not enter in the sample, the time shift of the first pulse observed for the different samples is only due to the different position of their upper surfaces Δh, i.e. to their thicknesses difference; the thicker the sample, the sooner the pulse arrives. Therefore, if we consider as reference the position of the metallic plate, $\Delta h = d$ where d is the unknown thickness of a sample that can be written as:

$$\Delta h = d = \frac{c}{2\, n_{air}\, \cos\, \theta_{air}} \Delta t \qquad (2)$$

Where $\Delta t$is the delay between reflected peak pulse (region A) and the one used as reference, c the speed of the light, n_{air} the refractive index of air (n_{air} =1) and θ_{air} the incident angle. In our case, this angle is fixed by the commercial system we used (θ_{air}= 8°).

Using this "optical"method, we evaluated the thicknesses of various pellets made of different materials (maltose, glucose and HDPE) and different material powder quantities, and we compared with micrometer measurements as a classical reference method (see figure 4). A very good agreement is obtained between the thicknesses calculated from the THz pulse reflection measurements (dots) using equation (2), and mechanically measured (dashed lines), regardless of the material used to fabricate the pellet.

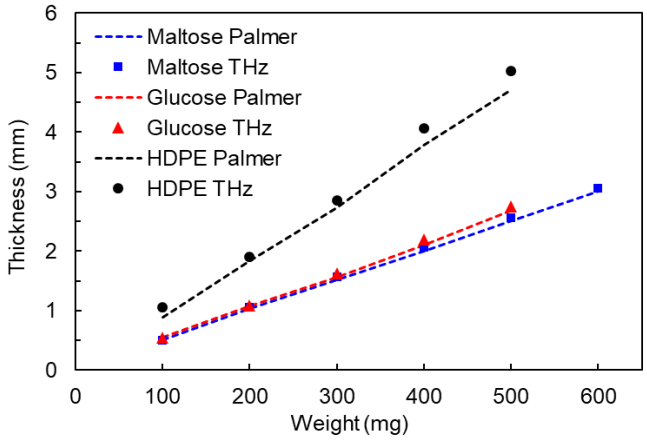

Figure 4: Comparison of samples thicknesses measured with palmer micrometer system (dashed lines) and evaluated using reflected THz pulses measurements (dots).

Thus, the thickness of a pellet can be easily calculated for each pixel in the image in order to plot the thicknesses image of each sample (see figure 5).

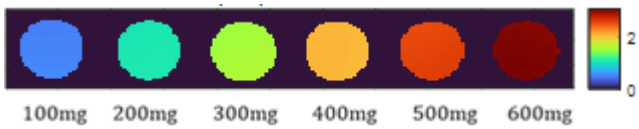

Figure 5: Thickness mapping of the 6 maltose samples, obtained from the first reflected pulse.

We can notice that this method does not depend on the material used to make the pellet as the THz signal is reflected at the top surface of the samples and does not propagate inside the sample. Thus, the signal peak position only depends on the sample thickness, as long as the material that constitutes the sample does not exhibit too much dispersion. Similar results have been obtained from the other samples made of glucose and polyethylene.

However, the time domain graph (Fig. 2) also shows a decrease in the amplitude of the peaks in the region A. Such a phenomenon would be expected if the refractive index of the material in the pellet changes, as predicted by equation (1). This is not the case here as all the tablets are made of pure maltose. One explanation could be related to a shift and/ or a change in size of the reflected beam on the receiver. In such cases, the receiver response would be affected and the measured reflected signal would vary depending on the thickness of the sample.

Indeed, when the THz pulse probes the sample under a given incident angle, the measured reflected signal will be delayed as explained previously but also a laterally shifted (Δx in Fig. 3) in comparison to the reference peak measurement, for which the reflected beam is fully centered at the surface of the receiver. According to figure 3,we can note that if the sample is probed under normal incidence θ_i= 0° and Δx=0. However, for the sake of simplicityof the optical setup, most of the available commercial THz imaging systems are using non-normal incidence experimental configuration in reflection. Moreover, imaging systems require focused THz beam (to get the smallest spatial resolution as possible) that can induce artefact of the same type when the reflection height varies, because of beam defocusing.

For these reasons, it is thus necessary to analyze and correct this geometrical issue created by a non-normal incidence and/or focused THz beam. The correction procedure is described in the following section.

3.2 Correction procedure and algorithm

Taking these undesired effectsinto account, the peak-to-peak amplitude E_{THz} of the reflected THz pulse is governed by the modulus of the Fresnel reflection coefficient (eq. 1). Onone hand, this depends only on the refractive index of the material that constitutes the sample under test, and on the other hand, by an error function f induced by the spatial shift Δx and the defocusing of the reflected beam as previously described(equation 3):

$$E_{THz}^{meas} = |R| \times f \times E_{THz}^{0}\,, \qquad (3)$$

where E_{THz}^{meas}, E_{THz}^{0}, are the peak-to-peak amplitude of the reflected and incident THz pulse respectively, |R| the modulus of the complex reflection coefficient, and *f* the error function induced by the misalignment and defocusing effects.

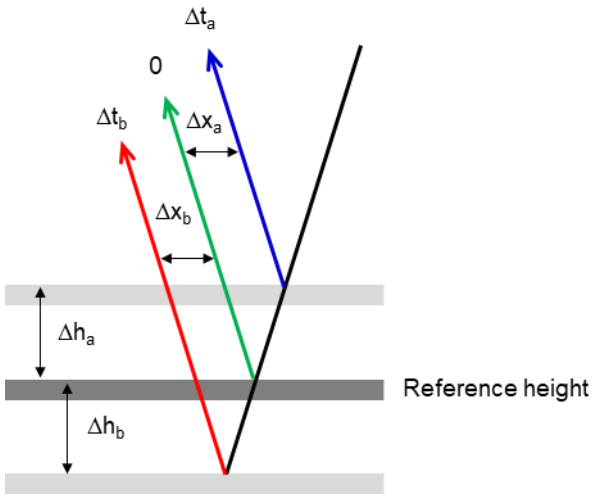

Figure 6: Representation of the lateral shift of the reflected beam for two different heights of the reflection surface.

To quantify the dreadful effect of the error function *f*, a calibration step is performed; for that the sample is removed and only the sample holder remains. As this holder is made of stainless steel, the THz pulse is totally reflected (|R|=1), and the pulse 2 (region B in Fig.2) disappears. By changing the vertical position of the reference metallic plate, the reflected pulse is temporally delayed (Δ*t*) and its amplitude varies due to i) the lateral shift (misalignment) and ii) defocusing of the reflected THz beam detected (see Fig. 6). On Fig. 7, we clearly illustrate this effect, by measuring the corresponding THz signal for two positions of the metallic plate, from both side of the reference one (in green). Thus, if the plate is moved above the reference level by using a translation stage, the time delay becomes shorter than the reference value. Whereas it is the opposite when the mirror is moved below the reference position.

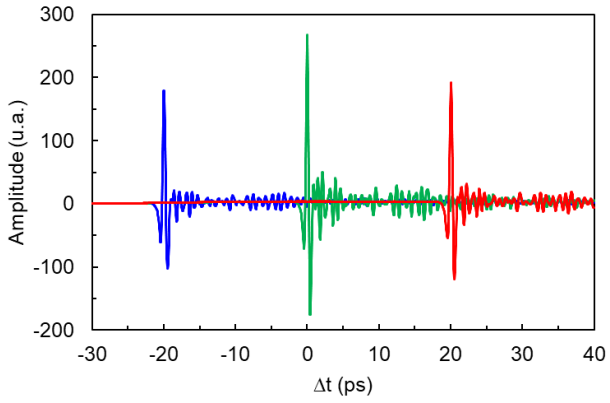

Figure 7: Respective quantitative impact on the delay and amplitude of the reflected THz pulse compared to the reference one (green).

The mirror height *Δh* can be calculated from the time difference Δ*t* between the peak positions of the corresponding THz signals with equation (2) and can be compared to the value given by the translation stage. Meanwhile, the parallel shift Δx on the receiver is given by:

$$\Delta x = 2\Delta h \cdot sin\theta_{air} \quad (4)$$

In our case, for the samples with the largest thickness (5 mm), this shift can reach 1.4 mm.

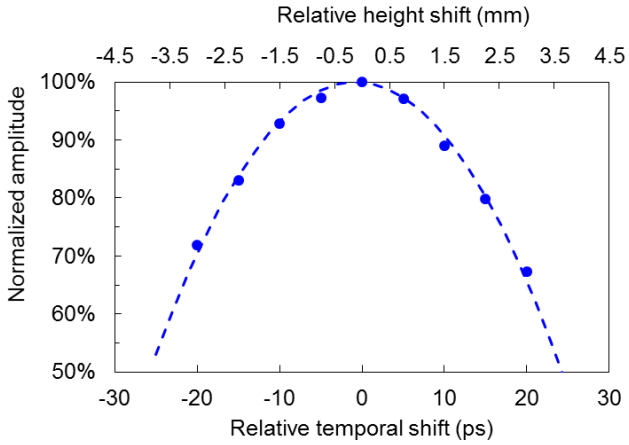

Figure 8: Modulation of the amplitude of the reflected THz pulse relative to the reference signal (at optimized position Δ*t* = 0) induced by misalignment and defocusing effects for different metallic plate positions (dots), and the associated parabolic fitting curve (dashed line).

The effect of such shift, and/or a beam defocusing is not very easy to predict theoretically, as it depends for example on the THz beam path in the optical system, on the THz beam interaction with the active area of the detector, etc. For that reason, we carefully and quantitatively investigated these effects on the THz pulse amplitude by varying the height of the stainless-steel holder. Fig. 8 represents the amplitude variation measured for the different heights of the reference plate (dots). As expected, the maximum amplitude is obtained at the reference position, whereas it decreases continuously when one deviates from it.

The error function *f* is then obtained by fitting the experimental results with a second order polynomial function (dashed curve in figure 8) relating to the equation below:

$$f = -8 \times 10^{-4}\,\Delta t^2 + 1.2 \times 10^{-3}\,\Delta t + 1 \quad (5)$$

3.3 Corrected amplitude and image

Equation (5) has then been used to correct the bare amplitude measurements (Fig. 2) obtained on the samples with different thicknesses. Fig. 9 shows the corrected results for the maltose tablets. We can see that the varying values of the peak amplitude has been greatly decreased compared to region A of Fig. 2. After correction, the THz pulse amplitude keeps roughly constant with a variation of the order of 3% at most, against 30% before correction, if we exclude the results obtained from the thickest sample. For the thicker pellet, the corrected result is not in agreement with the others, whereas the correction function keeps being valid for these ranges of thicknesses (see Fig. 8). Such artefacts can originate from the sample geometry (not

perfectly parallel faces), its orientation on the metallic plate holder etc.

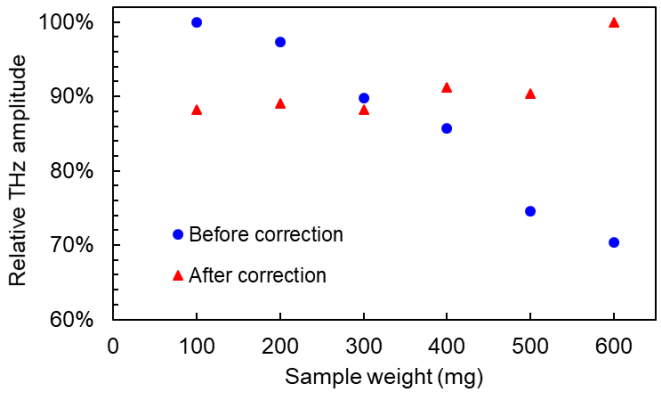

Figure 9: Corrected amplitude of the measured THz pulses for maltose pellets (red) compare to bare results (blue).

Finally, this correction process of the THz reflected amplitude has been applied on all the pulses corresponding to all the pixels of each image (Figure 10 b).

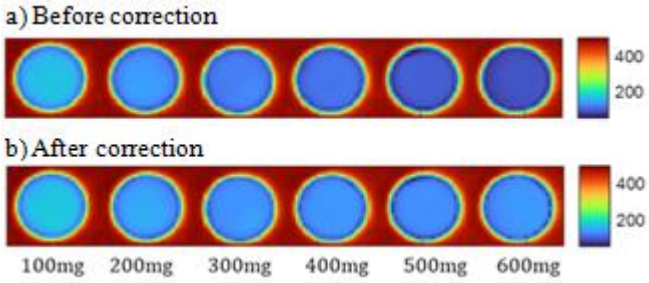

Figure 10: Non-corrected (a) and corrected (b) amplitude map of the 6 maltose samples.

By comparing Fig. 10.a and 10.b, we can see that the decreasing of the amplitude variation induced by the THz beam misalignment tends to homogenize the color of the different images, as expected for samples made of the same material.

Such a method can then be applied to verify the homogeneity of a sample or the presence of a sample with different composition, by using THz reflection. Indeed, as the THz reflected amplitude is directly linked to the refractive index of the material of the sample (equation 1), it can be used after correction, as a direct and reliable criterion to detect a change of composition of a given sample compared to a reference one.

4. Conclusion

The thickness measurement of chemical compound pellets can be directly achieved by using the Terahertz time-domain spectroscopy experiment in a reflection configuration. Because of some artefacts induced by the variation of sample thicknesses (beam shift and defocusing effect), it becomes necessary to correct the bare results by a correction function, which depends on the THz system used and that can be empirically estimated through a calibration step. We validate this method on different material pellets (maltose, glucose, polyethylene) for which the impact of such artefacts have been decreased by a factor 10. One can easily apply this method to i) extract the sample thickness without any contact with the sample, and ii) compare samples showing different topology. This also leads to saving a lot of time because no particular sample preparation is needed. The future work will include a large variety of materials and will be used to create a database of the targeted chemicals for future materials, mixture identification. In addition, in order to better discriminate chemical products, a similar approach will be performed in the frequency domain that would allow to obtain better performance, for example, on material exhibiting specific signatures in the THz frequency range.

Acknowledgements
The authors thank the CNRS (National Center for Scientific Research, France). All the THz measurement have been performed on the characterization platform PLATERA (https://www.platera.tech/).

Funding
NATO Science for peace (GS-5973).

Competing interest
There are no conflicts to declare.

References

[1] Ajito K., Yuko U. THz chemical imaging for biological applications. IEEE Transactions on Terahertz Science and Technology, 2011, **1.1**, 293-300.
[2] Shen Y. Terahertz pulsed spectroscopy and imaging for pharmaceutical applications: A review." International journal of pharmaceutics., 2011,**417**, 48-60.
[3] Lee W., Wangjoo L. Food inspection system using terahertz imaging. Microwave and Optical Technology Letters., 2014,**56.5**, 1211-1214.
[4] Federici J.F.,SchulkinB., HuangF., GaryD., BaratR., OliveiraF., ZimdarsD. THz imaging and sensing for security applications—explosives, weapons and drugs. Semiconductor Science and Technology., 2005, **20**, 266-280.
[5] Ellrich F., Bauer M., Schreiner N., Keil A., Pfeiffer T., Klier J., Weber S., Jonuscheit J., Friederich F., MolterD.Terahertz quality inspection for automotive and aviation industries." Journal of Infrared, Millimeter, and Terahertz Waves.,2020, **41.4**, 470-489.
[6] Miles R., Zhang X.-C., Eisele H., Krotkus, A. Terahertz Frequency Detection and Identification of Materials and Objects. Dordrecht: Springer Netherlands. 2007.
[7] Demers J. R. " UAV-mounted THz spectrometer for real-time gas analysis." SPIE 10531, Terahertz, RF, Millimeter, and Submillimeter-Wave Technology and Applications XI, 105310K (23 February 2018) 2018.
[8] Lavastre O., Pinault N., Mincheva Z. Organometallic Combinatorial Chemistry. NATO Sciences Series ASI, Principles and Methods for Accelerated Catalyst Design. Kluwer Academic Publishers., 2001, 135-151.
[9] Gaudry JB., Capes L., Langot P., Marcen S., Kollmannsberger M., Lavastre O., Freysz E., Letard JF., Kahn O. Second-order non-linear optical response of metallo-organic compounds: towards switchable

materials". Chem. Phys. Lett., 2000, **324 (5-6)**, 321-329.
[10] Chiang C.C, Wei M.T., Chen Y.Q., Yen P.W., Huang Y.C., Chen J.Y., Lavastre O., Husson G., Darsy G., A.Chiou, "Optical tweezers based active microrheology of sodium polystyrene sulfonate NaPSS", Opt. Express.,2011, **19(9)**, 8847-8854.
[11] Colin B., Lavastre O., Fouquay S., Michaud G., Simon F., Laferte O.,Brusson J.M. Development of new High-throughput screening method to compare and to detect efficient catalysts for adhesive materials. Int. J. Adhesion and Adhesive., 2016,**68**, 47-53**.**
[12] Colin B., Lavastre O., Fouquay S., Michaud G., Simon F., Laferte O.,Brusson J.M. Contactless Raman Spectroscopy-based Monitoring of Physical States of silyl-modifierd Polymers during Cross_Linking. Green and Sustainable Chemistry.,2016,**6**, 151-156**.**
[13] Lavastre O., Illitchev I., Dixneuf P.H., Jegou G., Oboyet T. Discovery of New Fluorescent Materials From Fast Synthesis and Screening of Conjugated Polymers. J. Amer. Chem. Soc., 2002,**124**, 5278-5279.
[14] Auston D.H., Cheung K.P. Coherent time-domain far-infrared spectroscopy. JOSA, 1985, B **2.4**, 606-612.
[15] Grischkovsky D., Keiding S., Van Exter M. Far-infrared time-domain spectroscopy with terahertz beams of dielectrics and semiconductors. JOSA, 1990, B**7.10**, 2006-2015.
[16] Duvillaret L., Garet F., Coutaz J.L.A reliable method for extraction of material parameters in terahertz time-domain spectroscopy. IEEE Journal of selected topics in quantum electronics., 1996,**2.3**, 739-746.
[17] Bernier M., Garet F., Kato E., Blampey B., Coutaz, J. L. Comparative study of material parameter extraction using terahertz time-domain spectroscopy in transmission and in reflection. Journal of Infrared, Millimeter, and Terahertz Waves, 2018, **39(4)**, 349-366.
[18] Bernier M., Garet F., Coutaz J.L. Determining the complex refractive index of materials in the far-infrared from terahertz time-domain data. Terahertz Spectroscopy-A Cutting Edge Technology., 2017, 119-141.
[19] Naftaly M., "Metrology issues and solutions in THz time-domain spectroscopy: Noise, errors, calibration". IEEE Sensors Journal., 2012, **13(1)**, 8-17.
[20] Bernier M., Garet F., Coutaz J.L., Minamide H., Sato A..Accurate characterization of resonant samples in the terahertz regime through a technique combining time-domain spectroscopy and Kramers–Kronig analysis". IEEE Transactions on Terahertz Science and Technology., 2016,**6(3)**, 442-450.
[21] Bernier M., Garet F., Coutaz J.L. Precise determination of the refractive index of samples showing low transmission bands by THz time-domain spectroscopy". IEEE Transactions on Terahertz Science and Technology, 2013, **3(3)**, 295-301.